Research Square

Preprints are preliminary reports that have not undergone peer review.
They should not be considered conclusive, used to inform clinical practice,
or referenced by the media as validated information.

Growth hormone induces TNF-α in podocytes and contributes to monocyte-to-macrophage differentiation: Implications in Diabetic kidney disease

Anil Kumar Pasupulati (anilkumar@uohyd.ac.in)
University of Hyderabad https://orcid.org/0000-0001-9467-7650
Rajkishor Nishad
University of Hyderabad
Dhanunjay Mukhi
University of Hyderabad
Srinivas Kethavath
University of Hyderabad
Sumathi Raviraj
University of Hyderabad
Manga Motrapu
University of Hyderabad
Sreenivasulu Kurukuti
University of Hyderabad

Article

Keywords: Podocytes, Growth hormone, Diabetic nephropathy, TNF-α, Monocytes, Macrophages.

Posted Date: February 2nd, 2022

DOI: https://doi.org/10.21203/rs.3.rs-1212793/v1

License: This work is licensed under a Creative Commons Attribution 4.0 International License.
Read Full License

Abstract

Diabetes shortens the life expectancy by more than a decade, and the excess mortality in diabetes is correlated with the incidence of kidney disease. Diabetic kidney disease (DKD) is the leading cause of end-stage kidney disease. In human biopsies and experimental models of DKD, macrophage accumulation predicts the severity of kidney damage. The mechanism of macrophage accumulation in diabetic glomeruli, however, is unknown. Increased growth hormone (GH) levels in type 1 diabetes and acromegalic patients had deleterious effects on glomerular biology. GH-treated mice had significant podocyte injury, glomerulosclerosis as well as increased macrophages. This study investigated if human podocytes injured by a GH stimulus contributed to macrophage accumulation. Following GH treatment, TNF-α signaling was increased in podocytes, as determined by RNA-seq analysis. Conditioned media from GH-treated human podocytes induced differentiation of THP1 monocytes to macrophages. Depleting the TNF-α in conditioned media with neutralizing antibodies diminished the effect of conditioned media from GH-treated podocytes on monocytes. Conditioned media from GH-treated primary podocytes with depleted TNF-α levels fail to elicit monocyte-to-macrophage differentiation. Mice administered with GH displayed glomerular accumulation of macrophages, podocyte injury, and proteinuria. Renal biopsies from DKD patients demonstrated activated TNF-α signaling, macrophage accumulation, and fibrosis. Together, this study suggests TNF-α secreted by podocytes under the influence of GH could contribute to macrophage accumulation, thus eliciting adverse renal inflammation and impaired function. Our study suggests targeting GH and/or TNF-α signaling could be a therapeutic approach to combat DKD.

Introduction

Diabetic kidney disease (DKD) is responsible for about half of all new cases of end-stage kidney disease (ESKD)[1]. Histopathological features of DKD include accumulation of extracellular matrix (ECM), thickening of glomerular and tubular membranes, tubulointerstitial fibrosis, and glomerular sclerosis. Interstitial fibrosis is the hallmark of progressive chronic kidney disease (CKD) and it correlated with kidney failure. Fibrosis is characterized by activation and proliferation of myofibroblast, migration of leukocytes, and excessive deposition of ECM. Although, the traditional perspective of diabetic kidney injury blamed metabolic and hemodynamic variables, recent studies revealed that chronic inflammation is a cardinal factor implicated in the progression of diabetic nephropathy (DN) to ESKD[2,3]. Macrophages account for majority of leucocyte infiltration in the kidney and their accumulation is associated with progression and severity of kidney damage in experimental models[3,4]. The presence of macrophages in diabetic kidney biopsies predicts a deterioration in kidney function[5,6]. Macrophages are the major invading cells in diabetic kidneys, implying that these cells have a harmful role in the disease manifestation [7]. Glomerular recruitment of macrophages during the early phase of hyperglycemia contributes to expansion of mesangium in diabetic rats [8] and macrophages are acknowledged as the primary inflammatory cell involved in the early glomerular injury in the pathology of DN[9] . On the other hand, depletion of macrophages in kidney ameliorated inflammation, improved albuminuria, and

progression of DN[10]. Since, macrophage accumulation predicts declined kidney function, the stimuli that skew macrophages into kidney needs to be investigated. It is noteworthy that kidneys display most significant age-related changes with accumulation of macrophages of M1-proinflammatory phenotype[11,12].

Diabetes is characterized by upregulation of endocrine factors such as GH, glucagon, and cortisol and DKD is presented with intra-renal alterations in GH/GH receptor (GHR) axis[13-16]. Excess GH conditions, such as acromegaly, and transgenic mice with GH hypersecretion, caused severe structural and functional alterations in the kidney[14]. The pleiotropic effects of GH are elicited by its direct contact with the GHR found on target tissues, or indirectly via promoting the release of insulin-like growth factor-1 (IGF-1). GHR expression was observed in predominant glomerular cell types (podocytes and mesangial cells) and tubular segments[13,17,18]. Renotoxicity of GH, but not IGF-1 was exemplified by studies in transgenic mice that showed glomerular hypertrophy, podocyte hypertrophy, progressive glomerulosclerosis, and albuminuria[18,19]. Similarly, deleterious effect of GH on podocytes was elucidated in vitro using human podocytes. Podocytes exposed to GH undergo phenotypic conversion from epithelial to mesenchymal transition and mitotic catastrophe[20,21]. Though, our recent study demonstrated kidney fibrosis, interstitial infiltration of plasma cells, and proteinuria in GH-administered mice [22], the definite role of GH on infiltration of cells into glomerulus remains elusive.

Since we observed the infiltration of plasma cells in the GH-treated mice glomeruli, we hypothesize that podocytes injured by a GH could contribute to the infiltration of these cells. Therefore, we performed RNA-seq analysis of GH-treated human podocytes to gain a comprehensive understanding of podocyte transcriptome and how GH affects podocytes and glomerular biology. TNF-α was activated in podocytes exposed to GH, and conditioned medium from GH-exposed podocytes induce monocytes differentiation to macrophages. With the showing of GH-dependent production of TNF-α and related glomerular macrophage infiltration, our study elucidates the functional consequences of novel GH action, resulting in altered glomerular physiology and function.

Materials And Methods

Antibodies and reagents:

The TNF-α (NBP1-19532), TNFR1 (NBP1-97453), CD11b (NB110-89474), MCP1 (NBP2-22-115), Podocin (NBP2-75624) and Nephrin (NBP1-77303) were purchased from Novus Biologicals (Minneapolis, Minnesota). The NF-kb (ab32536), pIKB-α (ab133462), IKB-α (ab32518), Lamin-B1(ab16048) were purchased from Abcam (Cambridge, MA); F4/80 from Biolegend (San Diego, CA); Phospho IKKa/b (ser176/180) (#2697), CD14 (D7A2T) (#56082) and β-actin (#4970) were from Cell Signaling Technology (Danvers, MA). CD68 Antibody (sc-17832) Santa Cruz Biotechnology (Dallas, TX). Mouse/Rabbit PolyDetector DAB HRP Brown Immunochemistry detection system (#BSB020, Santa Barbara, CA). Phalloidin fluorescein isothiocyanate labeled (#P5282), glutaraldehyde solution (G5882) and Giemsa stain (#26149-01) were obtained from Sigma Aldrich (St. Louis, MO, USA). Precision Plus

Protein Dual Color Standards (Bio-Rad, Hercules, CA) and ProLong™ Diamond Antifade Mountant (#P36961) were purchased from Molecular Probes Life Technologies. DyLight 488 and DyLight 564, and Cy5-conjugated secondary antibody were purchased from Vector Laboratories (Burlingame, CA). Primers used in this study procured from Integrated DNA Technologies (Coralville, IA). JAK2 inhibitor (AG490) were purchased from Tocris Bioscience (Pune, India). Human TNF-α Recombinant Protein (#PHC3015) TNF-α ELISA kit (#KHC3011) and MCP1 ELISA kit (#BMS281INST) were purchased from ThermoFisher Scientific. Paraformaldehyde (#P6148-500G), bovine serum albumin (BSA, A3294-50G), 4, 6-diamidino-2-phenylindole (DAPI, #P36971) were obtained from Sigma Aldrich (St. Louis, MO, USA).

Podocyte culture and treatment:

In this study, conditionally immortalized human podocytes (a gift from Prof. Moin Saleem, University of Bristol) cells were cultured essentially as described earlier[21]. Briefly, after 14 days of differentiation at 37°C, podocytes were treated with or without GH and GH + AG490. Unless otherwise mentioned, all the experimental conditions for podocyte cells were given for 1 h. The cell lysate was prepared for RNA isolation, immunoblotting, and enzyme-linked immunosorbent assay. For immunofluorescence, cells were cultured on coverslips, followed by treatment as mentioned above, subsequent fixation with paraformaldehyde (4%), and blocking with PBS containing normal BSA (5%) before incubation with primary antibodies. The next day, the samples were incubated with Alexa Fluor-conjugated secondary antibodies, and DAPI for nuclear stain, for 1 h at room temperature. Images were acquired using a laser scanning microscope (ZEISS, Germany). For F-actin staining in podocytes cells essentially as described earlier [22]. Podocytes were incubated with Phalloidin fluorescein isothiocyanate labeled (#P5282) for 40 min at room temperature. Next counterstaining by DAPI, mounting and images were acquired using a Leica trinocular microscope or Apotome Axio Imager Z2 (Zeiss). We analyzed images using LASX Industry Software and ImageJ (NIH).

RNA extraction, library construction, sequencing and analysis:

Total RNA was isolated from with or without GH treated HPC cells using Trizol (Invitro-gen#15596026) according to manufacturer instructions. RNA was further purified using a commercially available kit (RNeasy Mini Kit, QIAGEN). 20 µg of purified RNA from each sample was treated with 10 Units of DNase1 (Ambion TURBO DNase, Life Technologies) and further purified by using G Sure cell culture RNA isolation kit. From each RNA sample, Ribosomal RNA was removed using Ribo-Zero kit (NEB#E6310L), and further mRNAs were enriched using Oligo (dT) beads. Illumina paired-end library was prepared as per the NEBNext® Ultra™ RNA Library Prep Kit (NEB#E7530S). The paired-end libraries were prepared and sequencing performed using Illu-mina HiSeq-2500 sequencing platform. The resultant raw reads were compressed to fastq.gz format and deposited in GEO repository (GSE140308). The raw reads quality check report was generated and trimmed the reads as per the fastQC report. Trimmed reads were aligned to the human hg38 reference genome (GRCh38) using TopHat v2.1.0. The mismatch parameter along with all other parameters were set to default.

Gene expression quantification was performed using 'Cufflinks' tool and derived Fragments per Kilobase exon per million reads sequenced (FPKM) values. Differentially expressed genes were derived using 'Cuffdiff' tool a log2 Fold change value of ≥ 1 is taken as a cutoff to define upregulated and a value of ≤ -1 to define downregulated genes with p-value threshold 0.001 to maintain statistical significance. KEGG pathway analysis was performed for differentially expressed genes using KEGG pathways and functional annotations performed using g:profiler tool. Expressed genes Venn diagram was generated using Ugent web tool (http://bioinformatics.psb.ugent.be/webtools/Venn/). Heatmap and volcano plots were generated using R programming. Gene Set Enrichment Analysis (GSEA) was performed using GSEA v4.1.0 software (Broad Institute).

Quantitative Real time PCR:

The total RNA was isolated from human podocytes and mouse podocytes using a TRIzol reagent. Next, 1 µg of total RNA was reverse transcribed using the cDNA synthesis kit (#6110 A, PrimeScript 1st strand cDNA Synthesis kit, TaKaRa). The qRT-PCR analysis was performed by the QuantStudio 3 system (Applied Biosystems) with SYBR Green (Kappa Biosystem) Master Mix as mentioned in the following protocol: initial denaturation at 95 °C for 3 min, followed by 35 cycles of three steps each at 95 °C for the 30 s, 60 °C for 30 s, and 72 °C for 30 s. The expression levels of β-actin did not change under the different experimental conditions and were used as an internal control to normalize each gene's mRNA expression. The primers and siRNA sequence used are shown in Supplementary Table.1.

THP1 cell culture and treatment:

THP-1 cells were cultured as described earlier [23]. Cells were maintained at 37°C in an atmosphere containing 5% CO2. For exposure, the THP-1 monocytes were seeded in 12 well Corning™ Costar™ Flat Bottom Cell Culture Plates (Fisher Scientific Hampton, New Hampshire, USA) to a density of $5x10^5$ cells/mL in a volume of 1 mL and incubated for 24 h. To assess the impact on THP1 differentiation into macrophage, the cells were exposed to 50% of conditioned media (CM; prepared by adding spent media with fresh RPMI) from with or without GH treatment, GH+AG490 and from GH neutralizing CM and incubated for another 72 h to initiate differentiation into macrophage-like cells. The effect of CM from with or without GH and GH+AG490-CM to podocyte on THP1 differentiation into macrophages Giemsa staining was performed as recommended by the manufacturer protocol and image captured using EVOS M5000 cell imaging system (Invitrogen) light microscope. TNF-α neutralization in CM was performed as recommended by the manufacturer's protocol (#7321).

Animal and tissues:

Eight-week-old Swiss Webster male mice weighing 30±3 g were used. Mice were allocated randomly (not blinded) into to three groups: (1) control group, (2) GH-treated group and (3) GH + AG490. Mice received a single i.p. injection of hGH (1.5 mg/kg) or an equal saline volume per day for 6 weeks. We used a predefined value of n = 6 mice/group. The inhibitor group mice were received AG490 (1 mg/kg of b.w.) per day in addition to GH. If animal dies prematurely the data excluded from the analysis. After 6 weeks of

the experimental period, the mice were placed in individual metabolic cages for collecting 24 h urine to estimate albumin (#COD11573) and creatinine (#COD11502) levels, as recommended by the manufacturer's protocol (Biosystems, Barcelona, Spain). Disease establishment was confirmed by estimating the UACR. An aliquot of urine from mice was subjected to SDS-PAGE gel, and silver staining was performed to compare the urinary protein profile for all three groups. Further, we have also measured the GFR in these mice, as described previously[22]. Mouse podocytes were isolated from the kidney of mice, as described in earlier protocol[24]. Briefly, glomeruli were prepared by filtration of the kidney's cortex with mesh sieves, whose holes were 100, 76, and 54 µm in diameter. The tissues left on the mesh sieve with 54 µm holes were collected and prepared for the qRT-PCR and immunoblotting. For histological analysis, the kidney cortex was fixed with 4% paraformaldehyde before embedding in paraffin. Paraffin-embedded tissues were sliced longitudinally into 3–4 µm thick sections, subjected to staining with H&E and PAS staining. We obtained TEM images for glomerular sections from all the experimental mice groups described earlier[25]. The experiments with animals were approved by IAEC of University of Hyderabad, Hyderabad, India.

Flow cytometry analysis:

In order to confirm that CM from GH treated podocytes induces Cd11b differentiation marker from THP-1 cells to macrophages by flow cytometry. THP1 cells (2 x 10^6 cells/ml) are treated with or without CM from GH and GH+AG490 for 72 h. Cell surface staining were performed by direct immunofluorescent assay with fluorescence-conjugated CD11b antibody and corresponding isotype control antibodies for 30 min at room temperature in the dark. Next cells were centrifuge (500xg maximum) at 4^{O}C for 5 min and resuspended the pellet in 200 µl of PBS for flow cytometric analysis using S3e Cell Sorter flow cytometer (Bio-Rad). Data were analyzed using FCS Express 7 program.

Western blot analysis:

Cytoplasmic extract for immunoblotting was prepared as described previously [22]. Briefly, human podocytes and isolated mouse primary podocytes were lysed by RIPA buffer (#9806, Cell Signaling Technology) containing protease inhibitor mixture (#05056489001, Sigma Aldrich) and phosphatase inhibitor tablets (Roche), centrifuged and collected as supernatants. Nuclear protein extract for immunoblotting was prepared as described earlier [21]. Briefly, cell pellet was resuspended in nuclear extracting buffer and vortexed for 20 s. Incubate the cell lysate for 25 min on ice and vortex every 10 min for 10 s. Next, cell lysate was centrifuged for 12 min at 19,400xg at 4°C, and the supernatant (nuclear) was collected. The protein concentrations of cell and mouse podocyte lysates were determined using a bicinchonic acid reagent (ThermoFischer Scientific), using BSA as a standard. An equal amount of protein from corresponding samples was subjected (25-30 µg) to SDS-PAGE and immunoblotting, and bands were visualized using a ChemiDocTM XRS System (Bio-Rad, Hercules, CA).

Enzyme-linked immunosorbent assay:

The CM from with or without treated podocytes were collected for the detection of related indexes. The expressions of TNF-α and MCP-1 in CM were detected by ELISA. The operation was carried out according to the kit instructions (ThermoFischer Scientific) with the double antibody sandwich ELISA. Briefly, the only media, CM from podocyte with or without GH-Ab and GH-Ab+AG490 treatment for 1 h were collected and applied to TNF-α and MCP1 ELISA plates. Next washing and enzyme-labeled antibodies were added to combine with the antigen to form the enzyme-labeled antibody-antigen-solid antibody complex. Finally, substrate was added for color development, and the depth of color was measured at 450nm using a fluorescent microplate reader (Multiskan Microplate reader, ThermoFisher Scientific).

Chemotaxis assay:

The invasion of THP-1 cells was estimated using a modified method as described earlier [26]. Briefly, THP1 cells were spun down at 1000 rpm and resuspended in 1 ml of 0.1% BSA-RPMI. After adjusting the cell density to $1x10^5$ cells/ml, 2.5 ml of only media (CTL), CM from podocytes treated with or without GH-Ab or GH-Ab+AG490 were add to each 24 well plate. Next, the transwell insert was placed into the each 24 well plate (6.5 mm Transwell with 5-μm pore size, CLS3421-48EA; Corning, NY) with 10,000 cells in 100 μl incubated for 4 h at 37°C in an atmosphere containing 5% CO2. The insets were removed and migrated cell in the bottom well were transferred to 17x120 mm tube (#352096) and cell counting was performed using a FACScan (Becton-Dickinson, San Jose, CA).

Human kidney specimens:

Immunohistochemistry of human kidney biopsies were not performed for the purpose of this study, but collected from archived kidney biopsies without patient identifiers from Guntur Medical College, AP, India. Informed consent was obtained from the patients that these kidney biopsies obtained for patient care could be used for research purpose. The selected cases were with biopsy proven DN and proteinuria. This study was approved by the Institutional Review Board of Guntur Medical College and Government General Hospital, Guntur, Andhra Pradesh, India (application number GMC/IEC/120/2018). Our study protocols were abide by the Declaration of Helsinki principles.

Results

Transcriptomic profiling of GH treated human podocytes revealed activation of TNF-α signaling pathway:

To conduct an unbiased survey of putative direct targets of GH action (early response genes) we treated immortalized human podocytes for 30 min and performed RNA-seq analysis. Pearson correlation coefficient was calculated and found significance between replicates (**Fig.S1**). We performed whole transcript analysis and number of differentially expressed genes (>1 fold) were presented as volcano plot (**Fig.1A**). We analyzed the number of uniquely expressed genes in control and GH treatment and found that only 3330 genes were selectively expressed in podocytes exposed to GH (**Fig.1B**). Hierarchical cluster of differentially expressed genes between replicates of control and GH-treatment were presented as Heat map (**Fig.1C**). KEGG pathway analysis of up-regulated genes in GH-treatment revealed activation of TNF-

α pathway components and apoptosis (**Fig.1D**). Gene set enrichment analysis (GSEA) of the transcriptome of GH–treated podocytes revealed up-regulation of protein secretory pathway genes (**Fig.1E**).

GH induces TNF-α signaling in human podocytes:

We next validated our RNA-seq data by performing qRT-PCR and immunoblotting and found that GH induces TNF-α expression in human podocytes (**Fig.2A&B**). TNF-α is a pleiotropic cytokine, and by binding to TNF-receptor (TNF-R1), it exerts signaling cascades that are essential for induction of inflammation and modulation of immune responses. We then measured TNF-α associated inflammatory markers and found elevated expression of NF-kB, IL-1β, MCP1, CXCL1, and CXCL2 in human podocytes (**Fig 2A**).One of the significant downstream signaling events mediated by the TNF-α is the activation of the NF-kB. We observed activation of canonical NF-κB signaling in GH treated podocytes as evidenced by phosphorylation of IKK-α/β, IkB-α, and NF-kB (**Fig.2B & Fig.S2A)** and nuclear localization of NF-kB (**Fig.2C**). Interestingly, GH-induced expression of inflammatory cytokines and activation of NF-kB was attenuated in the presence of AG490, a specific and potent inhibitor of the JAK2, which transduces GH's effects (**Fig.2A-C**). Autocrine action of TNF-α secreted by podocytes under GH stimulus was verified by collecting conditioned media (CM) from GH-treated podocytes (GH-CM) and treated podocytes that were naive to GH. We found activation of TNF-R1 and NF-kB in podocytes exposed to GH-CM (**Fig.S2B**).

Inflammatory responses that manifest in progressive glomerulonephritis were presented with cytoskeletal abnormalities including podocyte foot-process effacement [27]. Inflammatory responses were also shown to elicit a transient reduction in F-actin [28]. Since we observed inflammatory response in podocytes exposed to GH, we determined F-actin distribution using FITC labeled phalloidin. Phalloidin staining revealed a significant reduction of stress-fibers in GH-treated podocytes (**Fig.2D&E**). In addition to the loss of stress fibers, we noticed decreased expression of slit-diaphragm components (nephrin and podocin) that are crucial for podocyte function when exposed to GH (**Fig.2F&G**). We tested the specificity of GH to alter podocyte stress fibers and slit-diaphragm proteins in the presence of AG490 (a JAK2 inhibitor), which abolishes GH action on target cells. AG490 prevented GH-induced aberrations in podocyte actin cytoskeleton and expression of slit-diaphragm proteins (**Fig.2D-G**).

Conditioned media from GH treated podocytes (GH-CM) elicits THP1 monocyte differentiation into macrophages:

Since TNF-α and MCP1 are secretary molecules, we confirmed that GH-CM possess TNF-α and MCP1 by performing ELISA (**Fig.3A&B**). It is interesting to note that in CM collected from podocytes that were treated with both GH and AG490, the levels of TNF-α and MCP1 were depleted (**Fig.3A&B**). Next, we tested the potential of GH-CM from podocytes to induce monocyte-to-macrophage differentiation. When compared with monocytes, macrophages are giant, granular, and invasive. THP1 monocytes that were treated with GH-CM showed increased cell size and granularity, characteristics features of macrophages, as analyzed by Giemsa's staining (**Fig.3C&D**). The potential of GH-CM to provoke monocyte-to-

macrophage differentiation is diminished when podocytes were treated with AG490 (**Fig.3C&D**). It is noteworthy that direct exposure of THP1 monocytes to GH did not elicit their differentiation to macrophages (**Fig.S3A&B**).

Further, we demonstrated paracrine action of GH on monocyte-to-macrophage differentiation by analyzing cell surface marker CD11b by FACS (**Fig.3E**). GH-CM from podocytes induced CD11b expression in THP1 cells suggesting differentiation to macrophages, whereas GH-CM from AG490 treated podocytes prevented CD11b expression in THP1 cells. Further monocyte-to macrophage differentiation was verified by increased expression of CD14 and CD68 in monocytes treated with GH-CM from podocytes (**Fig.3F**). Elevated expression of iNOS, TNF-α, MCP-1, and IL-1β, and decreased expression of Arginase1 suggest formation of M1 macrophages (**Fig.S3C**). Next, we performed a migratory assay using transwell filters and found that GH-CM induced enhanced migration, compared to CM from podocytes naive to GH treatment, or CM from podocytes treated with both GH and AG490 (**Fig.3G**). Monocytes treated with MCP-1 considered as a positive control. It is noteworthy that GH-CM neutralized with TNF-α antibody fail to elicit monocyte differentiation to macrophages (**Fig.3H&I)**.The data suggest that TNF-α in podocyte secretome elicits paracrine action on monocytes to differentiate into macrophages.

Essential Role of TNF-α in the effect of GH on monocyte to macrophage differentiation:

The above data suggest that CM from GH-treated podocytes consist of TNF-α elicited monocyte-to-macrophage differentiation. We then assessed the essential role of TNF-α to induce monocytes differentiation to macrophages by depletion of TNF-α in podocytes using siRNA. Mouse podocytes were isolated from healthy mice as described in methods section and transfected with siRNA for TNF-α or scrambled RNA. Immunoblotting confirmed the depletion of TNF-α in mouse podocytes transfected with siRNA **(Fig.4A)**. As evidenced by morphological changes, GH-CM from podocytes transfected with siRNA for TNF-α failed to induce monocyte to macrophage conversion **(Fig.4B)**. GH-CM from mouse podocytes transfected with siRNA for TNF-α curtailed the migratory potential of THP1 cells **(Fig.4C)**. We observed increased macrophage-specific CD14 and CD68 expression when treated with GH-CM from podocytes transfected with scRNA only, but not siRNA for TNF-α **(Fig.4D)**. Similarly, we noticed the elevated expression of M1 specific markers such as iNOS, MCP-1, and IL-1β **(Fig.4E)** in monocytes treated with GH-CM from podocytes in which TNF-α levels were unaltered. The data from primary mouse podocytes suggest the essential role of TNF-α in eliciting the GH-dependent transformation of monocytes to macrophages.

Activated TNF-α signaling in glomerular podocytes induced immune cell infiltration and proteinuria in GH administered mice:

Wenext validated in vitro observations of GH-induced activation of TNF-α signaling in mice administered with GH. Expression of TNF-α, NF-kB, IL-1β, IL-10, IkB-α, and MCP1 was significantly altered in podocytes isolated from GH-administered mice as analyzed by qRT-PCR (**Fig.5A**). Expression of TNF-α was significantly up-regulated in glomerular podocytes as analyzed by immunoblotting (**Fig.5B**) and immunohistochemistry (**Fig.5C**) in GH-administered mice. In contrast, supplementation of mice with

AG490 abrogated GH's effect on the expression of TNF-α and other inflammatory markers (**Fig.5A-C**). Tubular expression of TNF-α was also observed in GH-administered mice (**Fig.5C**). In tandem with elevated expression of TNF-α, we noticed significant infiltration of macrophages into the GH-injected mice glomeruli and interstitial as analyzed by H&E staining (**Fig.5D&D'**). We next verified the monocyte/macrophage origin of these infiltrated cells by staining for cell specific F4/80 staining. F4/80 staining was prominent in glomeruli from GH-administered mice (**Fig.5E&E'**). AG490 abolished GH-induced infiltration of macrophages into the interstitial and glomerular region (**Fig.5D&E**). We also observed glomerular fibrosis in the GH administered mice (**Fig.S4A-C**). We assessed the consequence of increased expression of TNF-α and accumulation of macrophage by evaluating kidney function. We observed proteinuria (**Fig.5F**), increased urinary albumin creatinine ratio (UACR) (**Fig.5G**), and declined glomerular filtration rate (**Fig.5H**) in mice administered with GH. Attenuation of GHR-JAK2 signaling by AG490 abrogated GH-induced kidney dysfunction. Impaired kidney function is concomitant with podocyte foot-process effacement in GH-administered mice as revealed by transmission electron microscopy (**Fig.5I**). In addition to podocyte injury, we also observed decreased podocyte number as assessed by WT1 staining (**Fig.5J&J'**). Together the data suggest that GH induces TNF-α in the podocytes and paracrine role of TNF-α could ensure macrophage infiltration thus compromise glomerular function.

TNF-α signaling is hyper activated in people with DN and presented with the accumulation of macrophages:

Finally, to confirm the data obtained so far that excess GH induces TNF-α signaling in humans, we evaluated the extent of inflammatory markers in healthy volunteers and people with DN. Initially, we used the Nephroseq database to assess the profile of inflammatory cytokines between non-diabetic (ND) and patients with DN. Expression of several chemokines and cytokines including CXCL1, CXCL5, IL17A, IL17RA, IL1B, IL6, IL8, MAP3K7, and TNF elevated in glomeruli from patients with DN (**Fig.6A**). Further, we found that expression of macrophage-specific markers such as CD14, CD68, CD163 and ITGAM was elevated in patients with DN (n=9) when compared with ND (n=15) volunteers (**Fig.6B**). We verified the biological significance of enhanced inflammatory markers in patients with DN by incubating podocytes with serum from ND and DN patients. Serum samples from DN patients have elevated TNF-α levels (**Fig.S5A**) and podocytes exposed to the serum from DN patients showed perturbations in podocyte cytoskeleton (**Fig.6C**).

Analysis of biopsies from DN patients revealed infiltration of immune cells into interstitium and glomerulus (**Fig.6D&D'**). Immunohistochemical analysis of the kidney sections from people diagnosed with DN showed increased glomerular NF-kB (**Fig.S5B**), TNF-α, and CD11b staining (**Fig.6E,F&S5C,D**), suggesting enhanced glomerular TNF-α and NF-kB staining correlates with increased macrophage population. We also observed fibrosis in the glomerular region of DN patients as evidenced Mason's trichrome staining (**Fig.6G&S5E,F**). These histological alterations in glomeruli from patients DN is paralleled with impaired kidney function as evidenced by proteinuria (**Fig.6H**), increased UACR (**Fig.6I**), and impaired estimated glomerular filtration rate (**Fig.6J**). All these data confirm that people with DN have elevated TNF signaling in their kidney glomeruli and accumulation of macrophages.

Discussion

Diabetes is presented with the recruitment of macrophages into the glomerulus even in the early stages of DKD[29]. Growing evidence suggests that podocyte injury plays an essential role in the pathogenesis of DKD[30]. Since altered GH levels are in diabetes are implicated in glomerular pathology, and glomerular podocytes express GHR, we investigated the early effect of GH on podocytes by performing RNA-seq. The predominant pathways affected by GH are TNF-α signaling, apoptosis, and cell adhesion pathways. Our data illustrate that GH elicits TNF-α secretion in podocytes, altering actin cytoskeleton and suppressing slit-diaphragm proteins. Conditioned media from GH-treated podocytes ensures the differentiation of THP1 monocytes into M1 macrophages (Fig. 7). Administration of GH in mice demonstrated macrophage accumulation in the glomerular region, which is concomitant with podocyte injury and proteinuria, a common symptom associated with DKD. Kidney biopsies from DKD patients revealed TNF-α signaling, macrophage accumulation, and fibrosis. Our study establishes that GH alters the podocytes' cytokine profile and consequently modulates monocyte transformation to M1macrophages and we speculate that paracrine action of GH could be the reason for observed inflammation and sclerosis in the settings DKD.

Under physiological conditions, the direct effects of GH include regulation of metabolism, fluid homeostasis, and blood pressure. Elevated GH levels in humans (acromegaly) presented with significant structural hitherto functional changes in the renal system. Studies of the GH transgenic mice[31], GH antagonist transgenic mice[32], and pharmacological blockade of the GHR [33] revealed a more direct involvement of GH/GHR axis in the pathogenesis of DN[13–16, 34]. An immediate action(s) of GH on the kidney was more evident upon the discovery of GHR and activation of canonical GH signaling cascade in podocytes[17]. In our earlier studies demonstrated the direct and IGF-1 independent action of GH on podocytes[17,20–22]. The direct effects of GH on podocytes include activation of Notch signaling[22], eliciting epithelial-to-mesenchymal transition[20], and mitotic catastrophe[21]. Besides TNF-α pathway, RNA-seq analysis revealed upregulation of apoptosis, adhesion junction, and cell-adhesion molecules in GH-treated podocytes, which reiterate our earlier observations where we performed PCR-array[35].

TNF-α is a prominent proinflammatory cytokine and its expression was shown to be elevated in the kidney of streptozotocin-indued diabetic rats[36]. TNF-α potently stimulates podocytes to produce MCP-1, and both TNF-α and MCP-1 levels were correlated with severity of albuminuria in diabetic *db/db* mice[37]. Importantly, TNF-α levels have been implicated in the development of renal hypertrophy during the early stage of DN[37]. TNF-α antagonist and anti-TNF-α antibody ameliorated renal hypertrophy and prevented albuminuria[37,38]. Urinary TNF-α levels independently correlates with glomerular and tubulointerstitial injury in type 2 diabetic patients [39] and severity of microalbuminuria[40]. Besides infiltrating inflammatory cells and podocytes, epithelial cells from proximal tubules are important sources of TNF-α in the kidney[41]. Enhanced TNF-α levels were observed in various forms of nephropathy including basement membrane nephropathy, obstructive nephropathy, cisplatin nephropathy, and DN[41]. The proportion of TNF-α secreted by each resident cell type of the kidney and any synergism in TNF-α secretion by resident cells, particularly podocytes and tubular epithelial cells, towards renal inflammation has yet to be determined.

A recent study reported that podocytes contribute and respond to the inflammatory milieu[42]. Microinflammation is the most important mechanism for the development and progression of DKD[9]. It was proposed that tissue macrophages responsible for renal remodeling whereas inhibition of macrophage accumulation prevents inflammation and offers renoprotection[9]. Macrophages, tissue effector cells of the monocyte lineage, are the significant part of recruited inflammatory cells in the inflammatory diseases of the kidney[43]. Macrophages were detected in the glomerulus and the interstitium in all inflammatory glomerular disorders. The population of macrophages is the predominant inflammatory cells in the kidney that outnumbers the lymphocytes, natural killer cells, and neutrophils[43]. The quantity of glomerular and interstitial macrophage population in the kidney correlates with poor outcomes such as disease progression and severity of presentation and the likelihood of fibrosis[44–47]. Single-Cell RNA Profiling of glomerular cells revealed that number of immune cells was significantly higher in diabetic glomeruli and these immune cells were predominantly macrophages[48].

Our study revealed that podocytes could secrete chemokines and cytokines and contribute to glomerular inflammation and sclerosis by activating macrophages upon exposure to GH. The ability of conditioned media from GH-treated podocytes to induce monocyte to macrophage transition may not be solely transduced by TNF-α since several other cytokines, including MCP-1, could activate macrophages. Our study did not rule out the possibility of contribution by other factor such as TGF-β in glomerular macrophage infiltration. TGF-β was also shown to promotes fibrosis by enhancing renal macrophage infiltration and deletion of TGF-bRII in macrophages prevented TGF-β1–mediated monocyte migration and macrophage chemotaxis[49]. The limitation of the study is we did not investigate the effects of macrophages on podocytes, even though we reported the paracellular effect of GH on monocytes to produce macrophages. It was shown earlier that macrophages provoke podocyte apoptosis[50]. Alternatively, undergoing class switching to inflammatory phenotype macrophages contributes to the activation of the inflammasome and activates fibrosis. Therapeutic strategies to prevent cellular transformation and inflammation could be translated into clinical treatments for diabetic complications. Since the prevention of GH action abolished TNF-α secretion, blocking GH/GHR axis or inhibiting macrophage activation could be therapeutic to combat diabetic kidney disease.

Declarations

Authors' contribution: RN, DM, AKP planned and designed the study. RN, DM, SR, and MM

performed the experiments. RN, DM, SK, SK, and AKP evaluated the data. RN and AKP wrote the manuscript. AKP obtained the funding.

Acknowledgments: The authors thank Dr. Rajasree Menon, University of Michigan for help analyzing RNA-seq data and Dr. Syed V Tahaseen for her help with human kidney specimens. AKP acknowledges Department of Health Research (12020/02/2019-HR), Science and Engineering Research Board (CRG/2019/5789), and University of Hyderabad (IoE/RC1-20-021).

Conflict of interest: The authors declare no competing interests.

References

1. Gregg, E. W. *et al.* Changes in diabetes-related complications in the United States, 1990-2010. *N Engl J Med* **370**, 1514-1523, doi:10.1056/NEJMoa1310799 (2014).
2. Navarro-Gonzalez, J. F., Mora-Fernandez, C., Muros de Fuentes, M. & Garcia-Perez, J. Inflammatory molecules and pathways in the pathogenesis of diabetic nephropathy. *Nat Rev Nephrol* **7**, 327-340, doi:10.1038/nrneph.2011.51 (2011).
3. Niewczas, M. A. *et al.* A signature of circulating inflammatory proteins and development of end-stage renal disease in diabetes. *Nat Med* **25**, 805-813, doi:10.1038/s41591-019-0415-5 (2019).
4. Chow, F., Ozols, E., Nikolic-Paterson, D. J., Atkins, R. C. & Tesch, G. H. Macrophages in mouse type 2 diabetic nephropathy: correlation with diabetic state and progressive renal injury. *Kidney Int* **65**, 116-128, doi:10.1111/j.1523-1755.2004.00367.x (2004).
5. Nguyen, D. *et al.* Macrophage accumulation in human progressive diabetic nephropathy. *Nephrology (Carlton)* **11**, 226-231, doi:10.1111/j.1440-1797.2006.00576.x (2006).
6. Yang, N. *et al.* Local macrophage proliferation in human glomerulonephritis. *Kidney Int* **54**, 143-151, doi:10.1046/j.1523-1755.1998.00978.x (1998).
7. Tesch, G. H. Macrophages and diabetic nephropathy. *Semin Nephrol* **30**, 290-301, doi:10.1016/j.semnephrol.2010.03.007 (2010).
8. Sassy-Prigent, C. *et al.* Early glomerular macrophage recruitment in streptozotocin-induced diabetic rats. *Diabetes* **49**, 466-475, doi:10.2337/diabetes.49.3.466 (2000).
9. Duran-Salgado, M. B. & Rubio-Guerra, A. F. Diabetic nephropathy and inflammation. *World J Diabetes* **5**, 393-398, doi:10.4239/wjd.v5.i3.393 (2014).
10. You, H., Gao, T., Cooper, T. K., Brian Reeves, W. & Awad, A. S. Macrophages directly mediate diabetic renal injury. *Am J Physiol Renal Physiol* **305**, F1719-1727, doi:10.1152/ajprenal.00141.2013 (2013).
11. Mukhi, D. & Susztak, K. The transcriptomic signature of the aging podocyte. *Kidney International* **98**, 1079-1081, doi:https://doi.org/10.1016/j.kint.2020.08.004 (2020).
12. Tabula Muris, C. A single-cell transcriptomic atlas characterizes ageing tissues in the mouse. *Nature* **583**, 590-595, doi:10.1038/s41586-020-2496-1 (2020).
13. Haffner, D., Grund, A. & Leifheit-Nestler, M. Renal effects of growth hormone in health and in kidney disease. *Pediatr Nephrol*, doi:10.1007/s00467-021-05097-6 (2021).
14. Pasupulati, A. K. & Menon, R. K. Growth hormone and chronic kidney disease. *Curr Opin Nephrol Hypertens* **28**, 10-15, doi:10.1097/MNH.0000000000000468 (2019).
15. Kumar, P. A., Brosius, F. C., 3rd & Menon, R. K. The glomerular podocyte as a target of growth hormone action: implications for the pathogenesis of diabetic nephropathy. *Curr Diabetes Rev* **7**, 50-55, doi:10.2174/157339911794273900 (2011).

16. Mukhi, D., Nishad, R., Menon, R. K. & Pasupulati, A. K. Novel Actions of Growth Hormone in Podocytes: Implications for Diabetic Nephropathy. *Front Med (Lausanne)* **4**, 102, doi:10.3389/fmed.2017.00102 (2017).
17. Reddy, G. R. *et al.* Identification of the glomerular podocyte as a target for growth hormone action. *Endocrinology* **148**, 2045-2055, doi:10.1210/en.2006-1285 (2007).
18. Doi, S. Q. *et al.* Growth hormone increases inducible nitric oxide synthase expression in mesangial cells. *J Am Soc Nephrol* **11**, 1419-1425, doi:10.1681/ASN.V1181419 (2000).
19. Blutke, A., Schneider, M. R., Wolf, E. & Wanke, R. Growth hormone (GH)-transgenic insulin-like growth factor 1 (IGF1)-deficient mice allow dissociation of excess GH and IGF1 effects on glomerular and tubular growth. *Physiol Rep* **4**, doi:10.14814/phy2.12709 (2016).
20. Kumar, P. A. *et al.* Growth hormone (GH)-dependent expression of a natural antisense transcript induces zinc finger E-box-binding homeobox 2 (ZEB2) in the glomerular podocyte: a novel action of gh with implications for the pathogenesis of diabetic nephropathy. *J Biol Chem* **285**, 31148-31156, doi:10.1074/jbc.M110.132332 (2010).
21. Nishad, R. *et al.* Growth hormone induces mitotic catastrophe of glomerular podocytes and contributes to proteinuria. *Cell Death Dis* **12**, 342, doi:10.1038/s41419-021-03643-6 (2021).
22. Nishad, R., Mukhi, D., Tahaseen, S. V., Mungamuri, S. K. & Pasupulati, A. K. Growth hormone induces Notch1 signaling in podocytes and contributes to proteinuria in diabetic nephropathy. *J Biol Chem* **294**, 16109-16122, doi:10.1074/jbc.RA119.008966 (2019).
23. Vemula, M. H. *et al.* Mycobacterium tuberculosis Zinc Metalloprotease-1 Assists Mycobacterial Dissemination in Zebrafish. *Front Microbiol* **7**, 1347, doi:10.3389/fmicb.2016.01347 (2016).
24. Murakami, A. *et al.* A novel method for isolating podocytes using magnetic activated cell sorting. *Nephrol Dial Transplant* **25**, 3884-3890, doi:10.1093/ndt/gfq323 (2010).
25. Nakuluri, K. *et al.* Hypoxia induces ZEB2 in podocytes: Implications in the pathogenesis of proteinuria. *J Cell Physiol* **234**, 6503-6518, doi:10.1002/jcp.27387 (2019).
26. Campbell, J. J., Qin, S., Bacon, K. B., Mackay, C. R. & Butcher, E. C. Biology of chemokine and classical chemoattractant receptors: differential requirements for adhesion-triggering versus chemotactic responses in lymphoid cells. *J Cell Biol* **134**, 255-266, doi:10.1083/jcb.134.1.255 (1996).
27. Kriz, W., Shirato, I., Nagata, M., LeHir, M. & Lemley, K. V. The podocyte's response to stress: the enigma of foot process effacement. *Am J Physiol Renal Physiol* **304**, F333-347, doi:10.1152/ajprenal.00478.2012 (2013).
28. Campos, S. B. *et al.* Cytokine-induced F-actin reorganization in endothelial cells involves RhoA activation. *Am J Physiol Renal Physiol* **296**, F487-495, doi:10.1152/ajprenal.00112.2008 (2009).
29. Thomas, M. C. *et al.* Diabetic kidney disease. *Nat Rev Dis Primers* **1**, 15018, doi:10.1038/nrdp.2015.18 (2015).
30. Reidy, K., Kang, H. M., Hostetter, T. & Susztak, K. Molecular mechanisms of diabetic kidney disease. *J Clin Invest* **124**, 2333-2340, doi:10.1172/JCI72271 (2014).

31. Doi, T. *et al.* Progressive glomerulosclerosis develops in transgenic mice chronically expressing growth hormone and growth hormone releasing factor but not in those expressing insulinlike growth factor-1. *Am J Pathol* **131**, 398-403 (1988).
32. Bellush, L. L. *et al.* Protection against diabetes-induced nephropathy in growth hormone receptor/binding protein gene-disrupted mice. *Endocrinology* **141**, 163-168, doi:10.1210/endo.141.1.7284 (2000).
33. Segev, Y., Landau, D., Rasch, R., Flyvbjerg, A. & Phillip, M. Growth hormone receptor antagonism prevents early renal changes in nonobese diabetic mice. *J Am Soc Nephrol* **10**, 2374-2381, doi:10.1681/ASN.V10112374 (1999).
34. Anil Kumar, P., Welsh, G. I., Saleem, M. A. & Menon, R. K. Molecular and cellular events mediating glomerular podocyte dysfunction and depletion in diabetes mellitus. *Front Endocrinol (Lausanne)* **5**, 151, doi:10.3389/fendo.2014.00151 (2014).
35. Chitra, P. S. *et al.* Growth Hormone Induces Transforming Growth Factor-Beta-Induced Protein in Podocytes: Implications for Podocyte Depletion and Proteinuria. *J Cell Biochem* **116**, 1947-1956, doi:10.1002/jcb.25150 (2015).
36. Mensah-Brown, E. P. *et al.* Streptozotocin-induced diabetic nephropathy in rats: the role of inflammatory cytokines. *Cytokine* **31**, 180-190, doi:10.1016/j.cyto.2005.04.006 (2005).
37. DiPetrillo, K., Coutermarsh, B. & Gesek, F. A. Urinary tumor necrosis factor contributes to sodium retention and renal hypertrophy during diabetes. *Am J Physiol Renal Physiol* **284**, F113-121, doi:10.1152/ajprenal.00026.2002 (2003).
38. Moriwaki, Y. *et al.* Effect of TNF-alpha inhibition on urinary albumin excretion in experimental diabetic rats. *Acta Diabetol* **44**, 215-218, doi:10.1007/s00592-007-0007-6 (2007).
39. Navarro, J. F., Mora, C., Muros, M. & Garcia, J. Urinary tumour necrosis factor-alpha excretion independently correlates with clinical markers of glomerular and tubulointerstitial injury in type 2 diabetic patients. *Nephrol Dial Transplant* **21**, 3428-3434, doi:10.1093/ndt/gfl469 (2006).
40. Lampropoulou, I. T. *et al.* TNF-alpha and microalbuminuria in patients with type 2 diabetes mellitus. *J Diabetes Res* **2014**, 394206, doi:10.1155/2014/394206 (2014).
41. Ramseyer, V. D. & Garvin, J. L. Tumor necrosis factor-alpha: regulation of renal function and blood pressure. *Am J Physiol Renal Physiol* **304**, F1231-1242, doi:10.1152/ajprenal.00557.2012 (2013).
42. Wright, R. D. & Beresford, M. W. Podocytes contribute, and respond, to the inflammatory environment in lupus nephritis. *Am J Physiol Renal Physiol* **315**, F1683-F1694, doi:10.1152/ajprenal.00512.2017 (2018).
43. Duffield, J. S. Macrophages and immunologic inflammation of the kidney. *Semin Nephrol* **30**, 234-254, doi:10.1016/j.semnephrol.2010.03.003 (2010).
44. Young, B. A. *et al.* Cellular proliferation and macrophage influx precede interstitial fibrosis in cyclosporine nephrotoxicity. *Kidney Int* **48**, 439-448, doi:10.1038/ki.1995.312 (1995).
45. Klessens, C. Q. F. *et al.* Macrophages in diabetic nephropathy in patients with type 2 diabetes. *Nephrol Dial Transplant* **32**, 1322-1329, doi:10.1093/ndt/gfw260 (2017).

46. Hill, G. S., Delahousse, M., Nochy, D., Mandet, C. & Bariety, J. Proteinuria and tubulointerstitial lesions in lupus nephritis. *Kidney Int* **60**, 1893-1903, doi:10.1046/j.1523-1755.2001.00017.x (2001).
47. Rovin, B. H., Doe, N. & Tan, L. C. Monocyte chemoattractant protein-1 levels in patients with glomerular disease. *Am J Kidney Dis* **27**, 640-646, doi:10.1016/s0272-6386(96)90097-9 (1996).
48. Fu, J. *et al.* Single-Cell RNA Profiling of Glomerular Cells Shows Dynamic Changes in Experimental Diabetic Kidney Disease. *J Am Soc Nephrol* **30**, 533-545, doi:10.1681/ASN.2018090896 (2019).
49. Chung, S. *et al.* TGF-beta promotes fibrosis after severe acute kidney injury by enhancing renal macrophage infiltration. *JCI Insight* **3**, doi:10.1172/jci.insight.123563 (2018).
50. Guo, Y. *et al.* Infiltrating macrophages in diabetic nephropathy promote podocytes apoptosis via TNF-alpha-ROS-p38MAPK pathway. *Oncotarget* **8**, 53276-53287, doi:10.18632/oncotarget.18394 (2017).

Figures

Figure 1

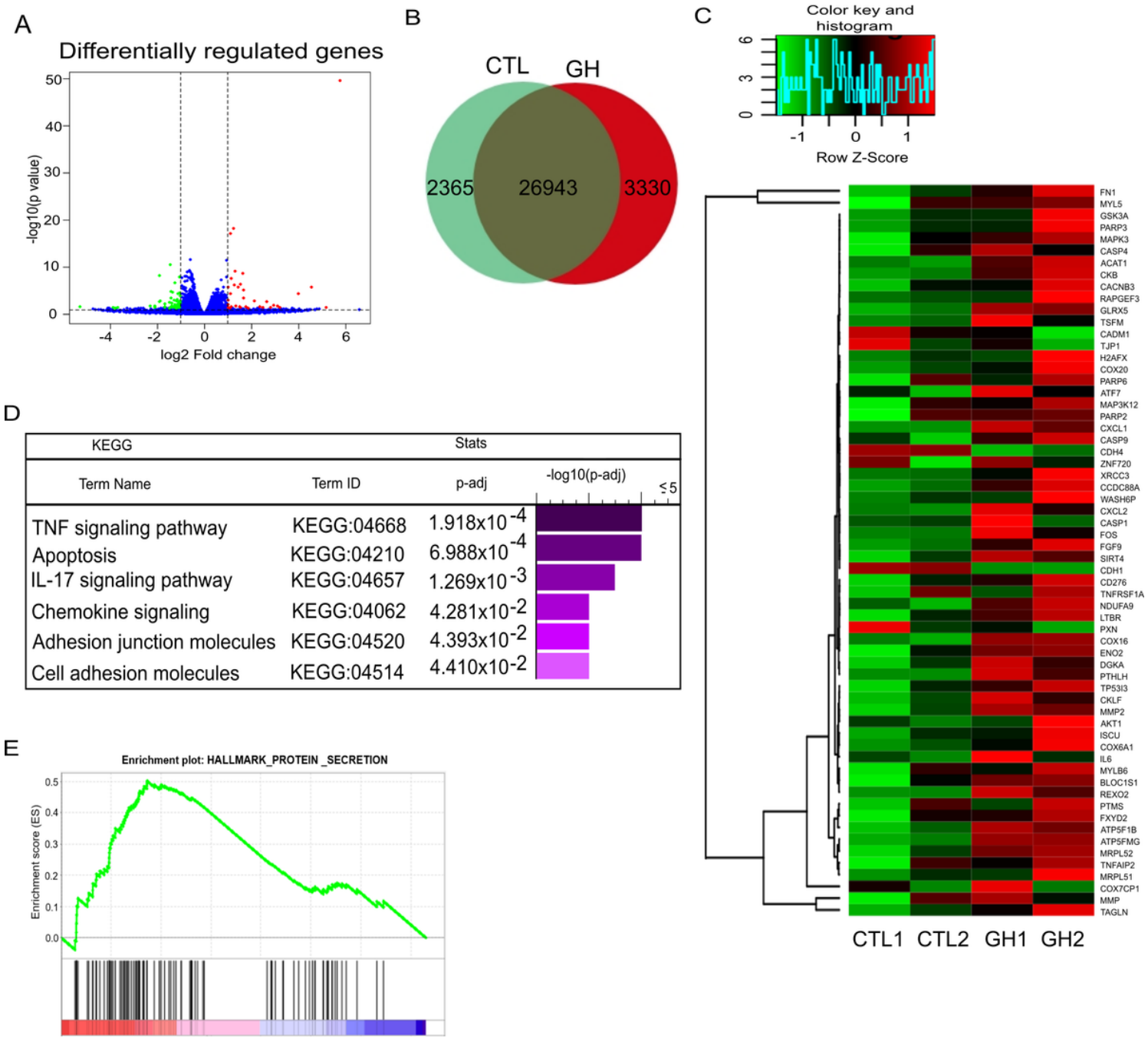

Figure 1

Gene expression profiling of Growth hormone (GH) treated human podocytes. Podocytes were treated with or without GH, and RNA-Seq was performed. **(A)** A volcano plot was generated using R programming by considering log2 fold-change against -log10 (p-value). Where red and green dots represent differentially upregulated and downregulated genes. $p<0.05$. **(B)** Venn diagram summarizing RNA-Seq data analysis shows the number of genes commonly expressed by podocytes with or without GH treatment. **(C)** Heatmap of 62 differentially expressed genes in podocytes with or without GH treatment conditions. **(D)** KEGG pathways are used for pathway enrichment analysis in podocytes with or without

GH treatment. **(E)** A significantly enriched secretory pathway enrichment plot was generated using the Gene Set Enrichment Analysis tool (GSEA 4.1.0).

Figure 2

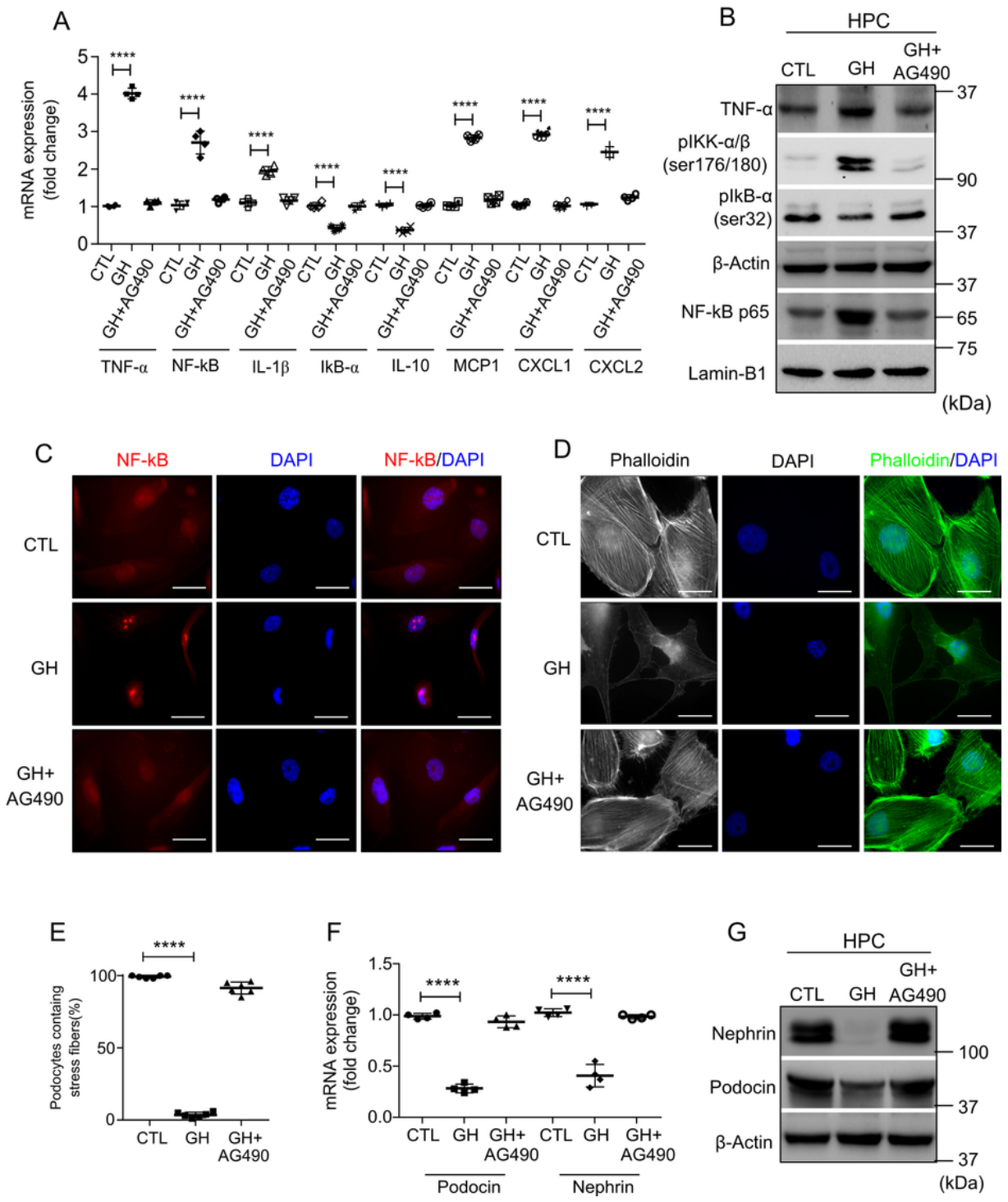

Figure 2

GH induces TNF-α mediated NF-kB activation in human podocytes. (A) qRT-PCR analysis showing the expression of TNF-α, NF-kB, IL-1β, IKKB, IL-10, MCP1, CXCL1, and CXCL2 in human podocytes treated with or without GH (500 ng/ml) and GH+AG490 (10 μM/ml) 30 min. β-Actin was used as an internal control. ****p<0.0001. **(B)** Immunoblotting analysis showing the expression of TNF-α, pIKK-α/β(ser176/180), pIkB-α(ser32), β-Actin, NF-kBp65, and Lamin-B1 in podocytes treated with or without GH (500 ng/ml) and GH+AG490 for 1 h. **(C)** Immunofluorescence analysis for NF-kB (red color) in podocytes treated with or without GH and GH+AG490 for 1 h. **(D)** Phalloidin staining of podocytes showing stress fibers (green color) in podocytes treated with or without GH and GH+AG490 for one hour. **(C&D)** DAPI (blue color) was used as a counterstain to visualize the nucleus. Scale bar=20 μm. Magnification = x630. **(E)** ImageJ quantifies Phalloidin-stained stress fibers in podocytes. Each dot represents the average value of twenty cells. n=6. ****p<0.0001. **(F&G)** mRNA and immunoblotting analysis showing the expression of nephrin, podocin, and β-Actin in podocytes treated with or without GH and GH+AG490 for 1 h. β-Actin and lamin-B1 served as an internal control. Data, presented as mean ±S.D. (n=3) and statistical significance was analyzed by one-way ANOVA post hoc Dunnett test.

Figure 3

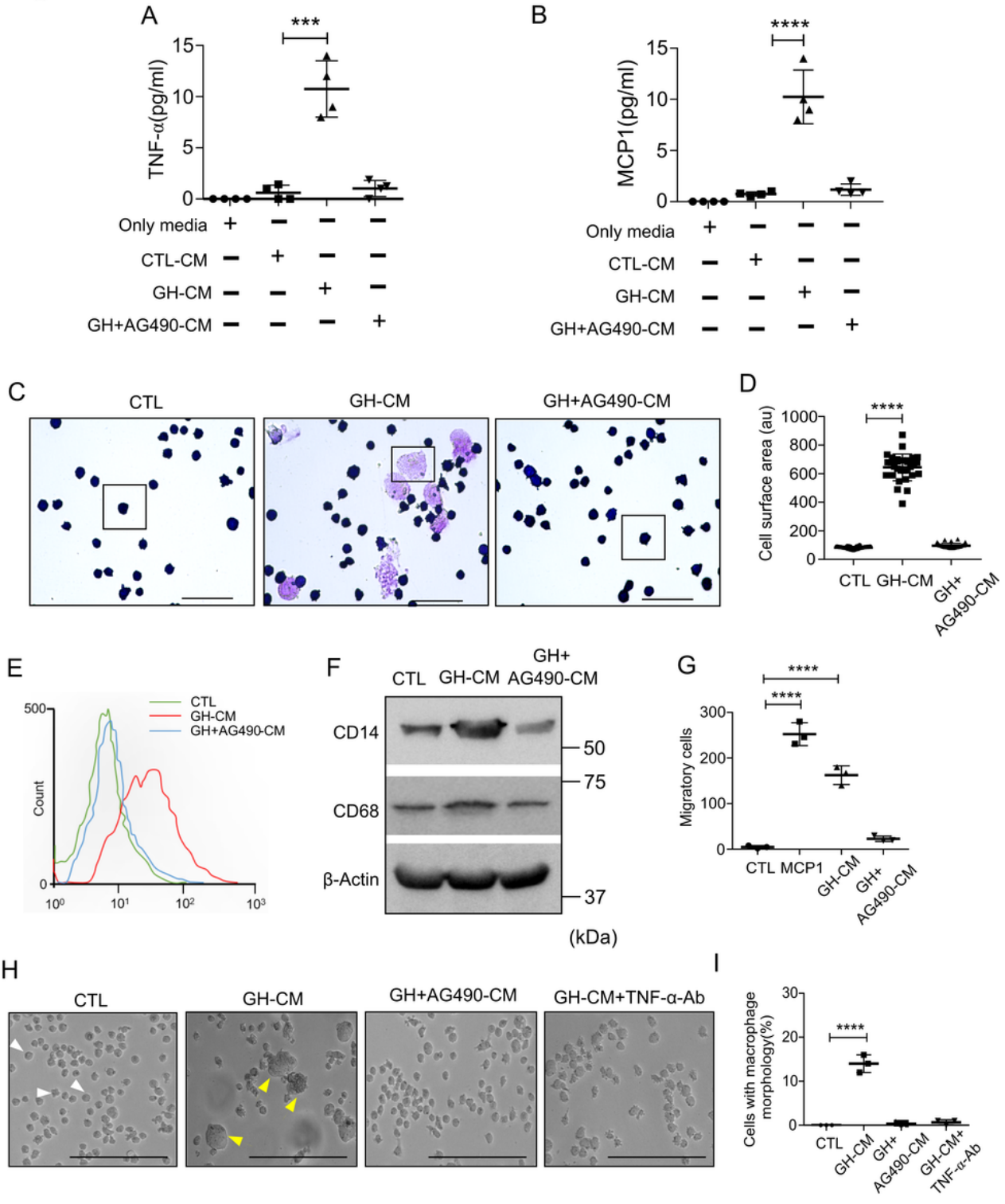

Figure 3

GH exposed podocytes CM activate THP1 cells differentiation into macrophages. (A&B) Quantification of TNF-α and MCP1 secretion in conditioned media (CM) from with or without GH and GH+AG490 treated human podocytes by ELISA. Only media was used as a negative control. ***p>0.002, ****P<0.0001. **(C&D)** Giemsa staining of THP1 cells without GH, GH-CM, and GH+AG490 treatment conditions. The highlighted area (black square box) representing a single cell, and cell surface area were

calculated from each experimental condition. (**D**). Each dot represented the value of a single cell surface area (n=30) and represented as an arbitrary unit (au) at Y-axis. ****p<0.0001. Scale bar=20µm. Magnification x600. **(E)** Flow cytometric analysis for expression of CD11b in THP1 cells from without GH, GH-CM, and GH+AG490 treatment conditions. **(F)** Immunoblotting analysis of CD14 and CD18 expression in THP1 cells treated with CM from GH-treated podocytes in the presence or absence of AG490. **(G)** Quantification of migratory cells (THP1) from the bottom of the well in without GH, GH-CM, GH+AG490-CM, and MCP1 experimental conditions using a FACScan (Becton-Dickinson, San Jose, CA). ****p<0.0001. **(H&I)** Light microscope images representing the morphological changes in THP1 cells after exposure with CM from with or without GH, GH+AG490, and GH-CM+ TNF-α-Ab treated podocytes. Scale bar 50µm. Magnification x400. Quantification of changes in THP1 cell morphology (white arrowhead indicates rounded appearance with monocytic morphology and the yellow arrowhead indicates fried egg with macrophage morphology) in with or without GH, GH+AG490, and GH-CM+ TNF-α-Ab treated podocyte CM. ****p<0.0001. (**I**) Each dot represents the average values of 10 areas from each experimental condition. Data presented as mean ±S.D. (n=3) and statistical significance was analyzed by one-way ANOVA post hoc Dunnett test.

Figure 4

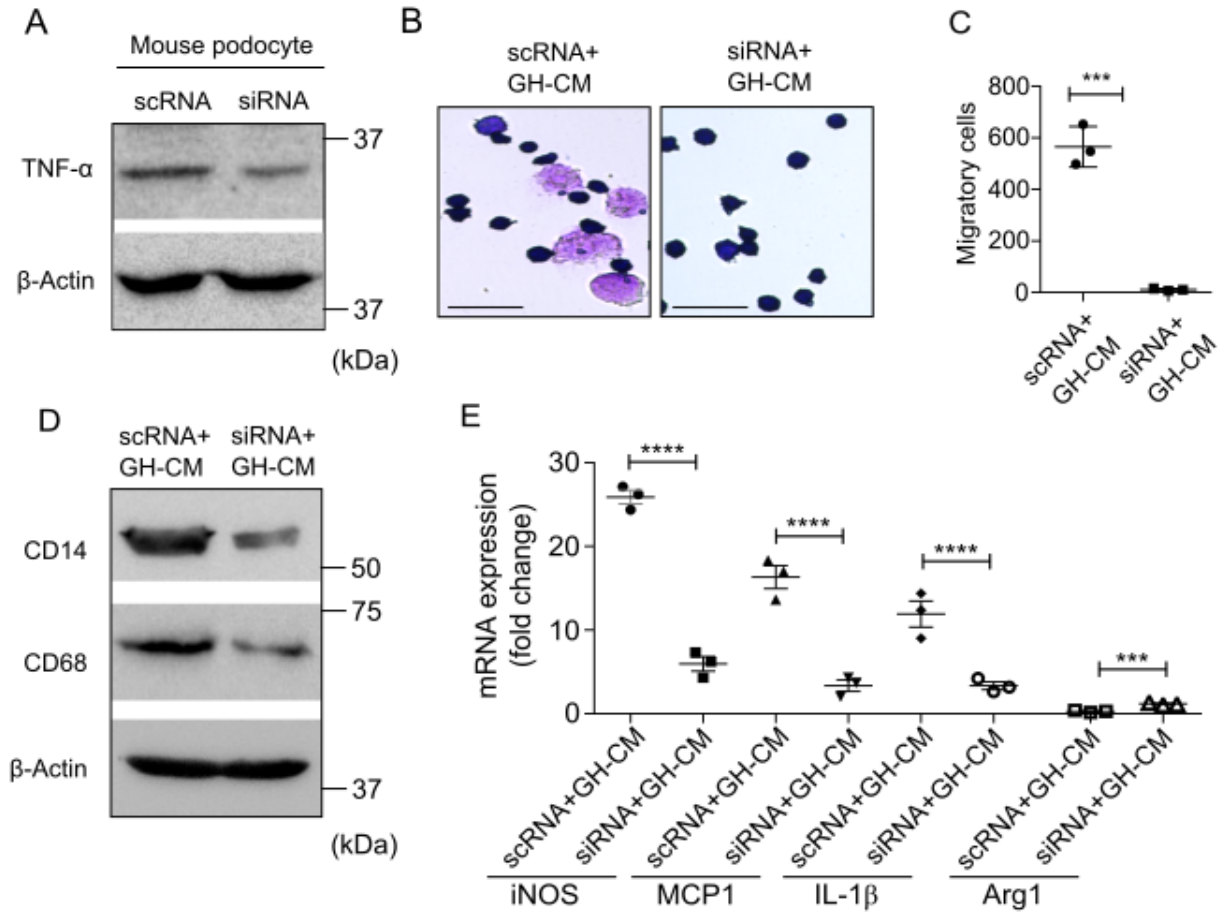

Figure 4

GH-induced TNF-α expression is essential for monocyte to macrophage differentiation. (A) Immunoblotting for TNF-α in mouse primary podocytes transfected with scrambled RNA (siRNA) or small interference RNA (siRNA) for TNF-. (**B**) Giemsa staining of THP1 cells treated with conditioned media (CM) from primary podocytes transfected with either siRNA or siRNA for TNF- and treated with GH. Scale bar=20μm. Magnification= x630. **(C)** Quantification of THP1 migration from the bottom of the well in scRNA+GH-CM and siRNA+GH-CM experimental conditions using a FACScan (Becton-Dickinson, San Jose, CA). ***p<0.001. **(D)** Immunoblotting analysis showing the expression of CD14, CD68, and β-Actin in THP1 cells treated with conditioned media (CM) from primary podocytes transfected with either scrambled RNA (scRNA) or siRNA for TNF- and treated with GH. **(E)** qRT-PCR analysis in THP1 cells for iNOS, MCP1, IL-1β, and Arg1 in scRNA+GH-CM and siRNA+GH-CM experimental conditions. ***p<0.001 and ****p<0.0001.

Figure 5

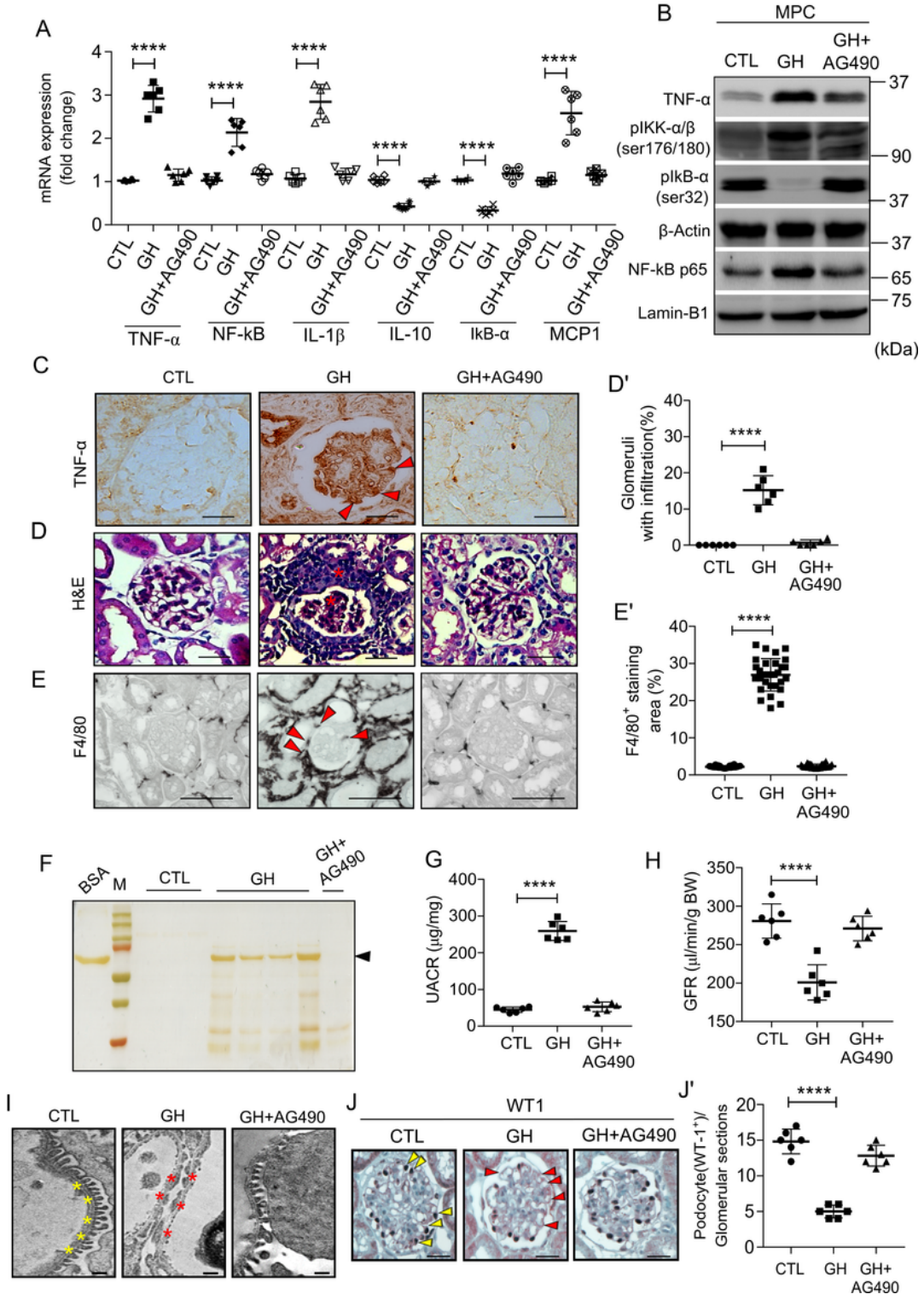

Figure 5

Activated TNF-α signaling is required for GH-induced immune cell infiltration and proteinuria. (A) qRT-PCR analysis of TNF-α, NF-kB, IL-1β, IL-10, IkB-α, and MCP1 in podocytes isolated from mice (MPC) ****p<0.0001. **(B)** Immunoblotting analysis showing the expression of TNF-α, pIKK-α/β (ser176/180), pIkB-α (ser32), β-Actin, NF-kBp65, and Lamin-B1 in MPC isolated from mice **(C)** Representative images of immunohistochemical staining for TNF-α (indicated by arrowhead in kidney sections from mice. Scale

bar=20μm. Magnification= x630. **(D)** Representative images of H&E staining in mice glomerular sections. Infiltrated cells are indicated by an asterisk. Scale bar=50μm. Magnification= x400. **(D')** The % of glomeruli with tubular interstitial immune cell infiltration was quantified and presented as a dot plot (right panel). ****p<0.0001. **(E)** Representative images of DAB staining for F4/80 in mice kidneys. The red arrowhead indicates the positive area along with the glomerulus. Scale bar=50μm. Magnification= x400. **(E')** The percentage of F4/80 positive area along with glomerulus quantified and presented as a dot plot (right panel). n=30. ****p<0.0001. **(F)** Urinary samples from experimental mice were subjected to SDS-PAGE and silver stained. Bovine Serum Albumin (BSA) was used as a reference marker. M-Protein marker. Arrowhead indicates a specific protein band for albumin. **(G&H)** Urinary albumin creatinine ratio (UACR) and glomerular filtration rate (GFR) were estimated with or without GH, and GH+AG490 treated mice group. ****p<0.0001. **(I)** TEM images of glomeruli from with or without GH and GH+AG490 treated mice group. Podocyte foot processes (yellow asterisk indicates healthy) effacement in GH treated mice indicated by a red asterisk. Scale bar= 0.5μm. **(J)** Representative images of immunohistochemical staining for WT1 (podocyte) in mice glomerular sections. Scale bars indicate 20 μm. Magnification=x630. Yellow arrowheadheads indicate the podocyte, and red arrowheads indicate capillaries devoid of podocytes. **(J')** The average number of WT1+ cells in the glomerulus of each mouse from with or without GH and GH+AG490 treated groups. We analyzed twenty-five glomeruli in each mouse, and average values represented as a dot plot. ****p<0.0001. Data, presented as mean ±S.D. (n=3) and statistical significance was analyzed by one-way ANOVA post hoc Dunnett test.

Figure 6

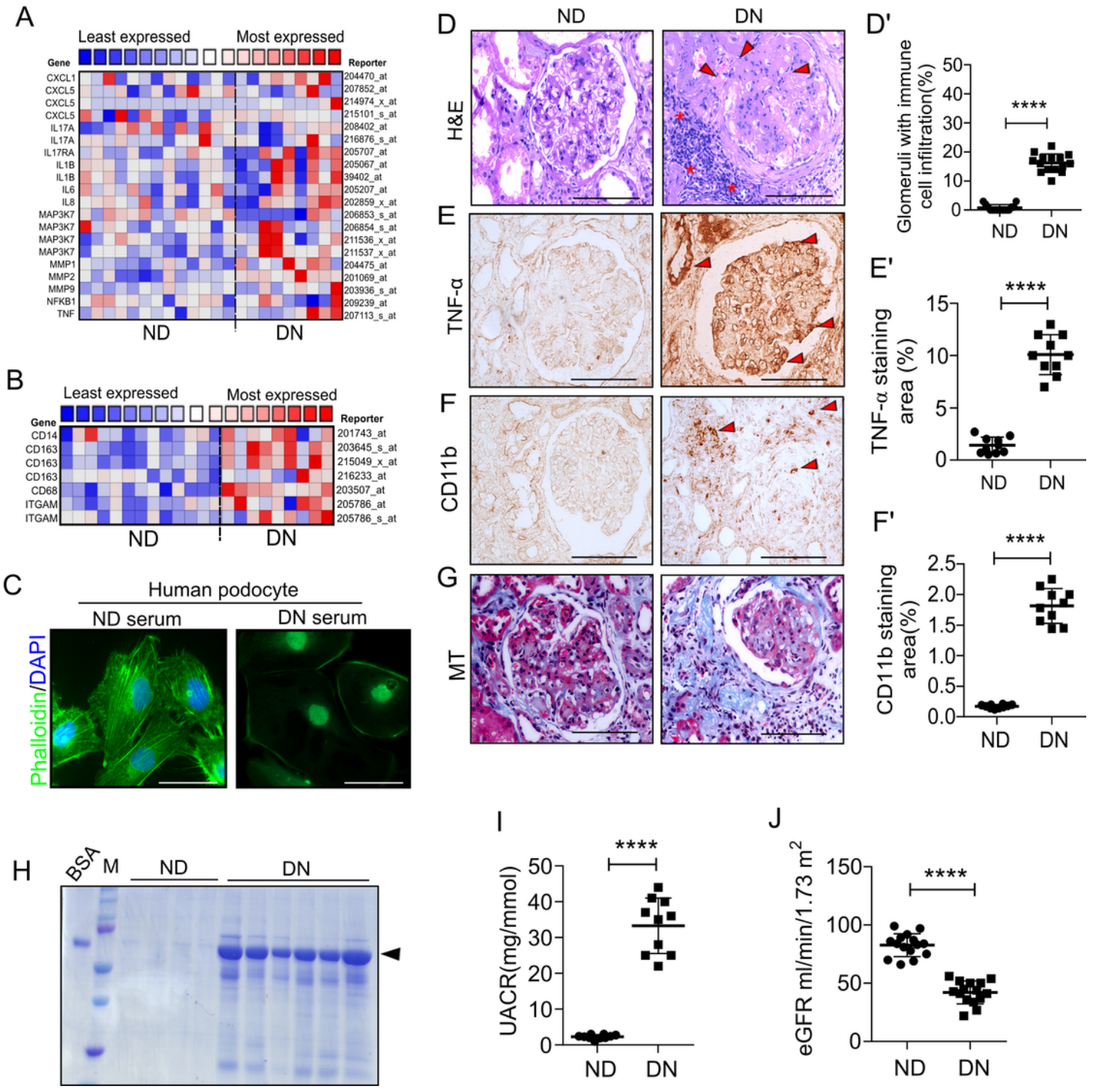

Figure 6

Elevated TNF-α signaling and activation of macrophages and proteinuria in DN patients. (A) Nephroseq (University of Michigan O'Brien Renal Center, Michigan, Ann Arbor, MI) analysis comparing CXCL1, CXCL5, IL17A, IL17RA, IL1B, IL6, IL8, MAP3K7, MMP1, MMP2, MMP9, NFKB1, TNF expression levels and **(B)** CD14, CD163, CD68 and ITGAM expression from non-diabetic nephropathy (ND, n=13) vs. diabetic nephropathy (DN, n=9) subject's glomeruli. Data indicate that expression of these genes

increased >1.5-fold in the DN. **(C)** Podocytes were treated with 10% sera from ND and DN subjects for 1 h, and phalloidin stain was performed. Magnification =x630. Scale bar=20μm. **(D)** Representative images of Hematoxylin & Eosin (H&E) staining in glomerular sections from ND and DN subjects. Interstitial immune cells (indicated by a red asterisk) and glomerular immune cells infiltration (indicated by red arrow) can be noticed in the DN subjects' glomerular section. Magnification= x400. Scale bar=50μm. **(D')** The percentage of glomeruli with tubular interstitial immune cell infiltration was quantified and presented as a dot plot (right panel). The total of five images from each subject (n=15) glomerular biopsy section and the average value presented as a dot plot (right panel). ****p<0.0001. **(E)** Representative images of immunohistochemical staining for TNF-α and **(F)** CD11b in glomerular sections from ND and DN subjects. Magnification x400. Scale bar = 50μm. Red arrowhead indicating specific expression of TNF-α, NF-kB, and CD11b. **(E'&F')** The percentage of staining area by TNF-α and CD11b (right panel) from a total of five images from each patient (n=10) glomerular biopsy section and the average values presented as a dot plot (right panel). **(G)** Representative image of Masson's trichrome (MT) Stain in glomerular sections from ND and DN subjects. Magnification x630. Scale bar = 20μm. **(H)** Urine samples from ND (n=3) and DN (n=6) subjects were resolved on SDS-PAGE and stained with Coomassie Blue. BSA was used as a standard control. M-standard protein marker. **(I)** Urinary albumin creatinine ratio (UACR). **(J)** Estimated glomerular filtration rate (eGFR) was measured in ND and DN groups. ***p<0.001. n=15 in both groups. Data are the mean± SD, and statistical significance was calculated using the student t-test.

Figure 7

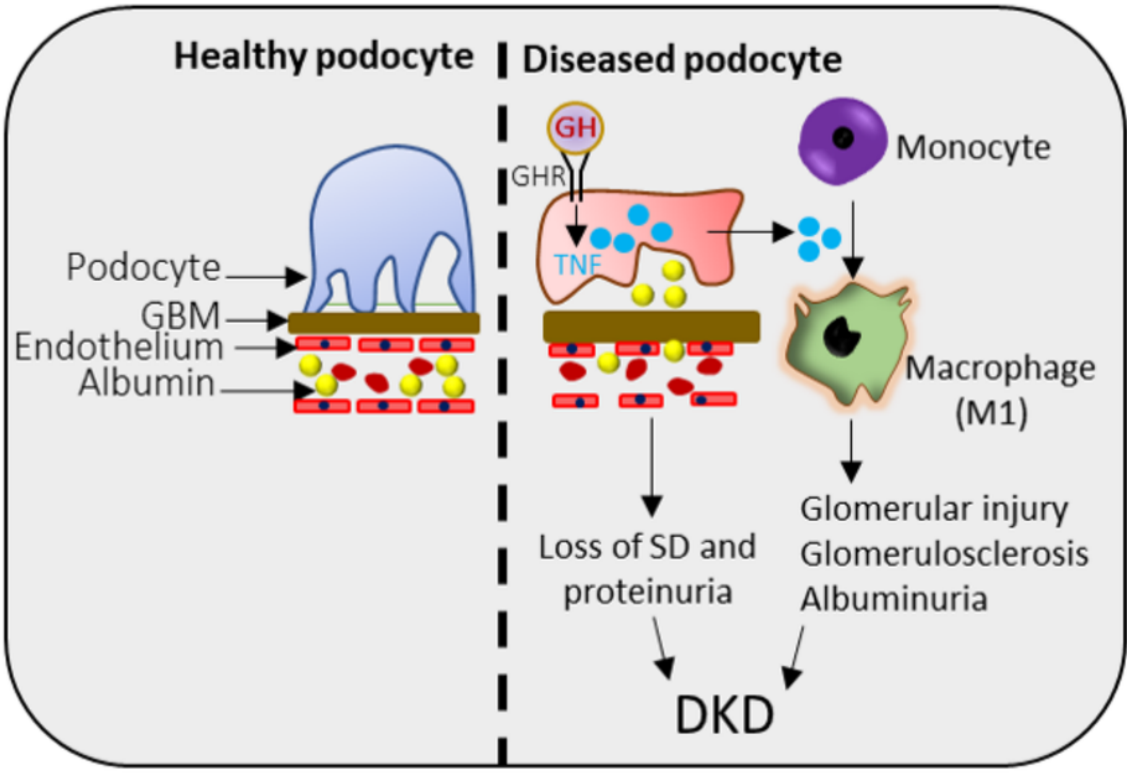

Figure 7

Schematic presentation of paracrine action of GH on podocytes to induce monocyte-to-macrophage differentiation.

Supplementary Files

This is a list of supplementary files associated with this preprint. Click to download.

- SupplementaryData1322.pdf